THEORETICAL STUDY OF RADIANT HEAT EXCHANGE FOR NON-GRAY NON-DIFFUSE SURFACES IN A SPACE ENVIRONMENT

NASA Research Grant: No. NGR-14-005-036

University of Illinois Budget Code: 46-22-40-356

Semi-Annual Status Report Number 2

Period Covered: August 1965 to February 1966

Prepared by: R. G. Hering
A. F. Houchens
T. Smith

Submitted by: R. G. Hering
Associate Professor of
Mechanical Engineering
266 Mechanical Engineering Bldg.
University of Illinois
Urbana, Illinois
Phone: Area Code 217, 333-0366

Date: February 1, 1966

Table of Contents

[redacted]

Nomenclature

a	correlation distance
$f(\psi,\pi;\theta,\phi)$	bi-directional reflectance of a perfectly conducting material for energy incident from (ψ,π) direction and reflected into (θ,ϕ) direction (Fig. 1)
$\rho(\psi,\pi;\theta,\phi)$	bi-directional reflectance for energy incident from (ψ,π) direction and reflected into (θ,ϕ) direction
$R(\psi)$	directional reflectance
$R(SP)$	specular reflectance
$\bar{R}$	normalized bi-directional reflectance
R_o	directional reflectance of a material with an optically smooth surface
σ	rms height of roughness elements
δ	Dirac delta function
ψ	polar angle of incidence
θ	polar angle of reflected beam
ϕ	azimuthal angle of reflected beam
$d\omega$	element of solid angle

Subscripts

λ	monochromatic quantity
c	coherent
ic	incoherent
i	incident
r	reflected

1. OBJECTIVES AND SCOPE

To evaluate the importance of such real surface radiating characteristics as non-diffuseness and non-grayness on the radiant heat transfer between surfaces in a space environment requires an acceptable description for the bi-directional reflectance of the participating surfaces. Some shortcomings of the Davies model for bi-directional reflectance of rough metallic surfaces which was expected to be used in this investigation were noted earlier [3]. Further study reported here suggests that the Davies model is not satisfactory for this study and a more satisfactory model is that of Beckmann. These two bi-directional reflectance models are discussed in Section 2.

2. RADIATION PROPERTIES FOR ROUGH SURFACES OF CONDUCTING MATERIALS

A general discussion of the affect of surface roughness and other surface characteristics has been given by Bennett [9]. The affect of surface roughness may be generally catagorized according to the magnitude of the optical roughness. As used here optical roughness refers to the ratio of a characteristic dimension of the surface asperity height to the radiation wavelength. For optical roughnesses much greater than unity, multiple reflections occur between the roughness elements resulting in increased emittance and decreased reflectance compared to those for the same material with an optically smooth surface. On the other hand, for optical roughnesses less than unity, the predominant influence of surface roughness on the radiation properties can be attributed to diffraction effects.

A general accounting of the interaction of an electromagnetic wave with a material boundary requires the solution of a system of partial differential equations and associated boundary conditions. Except for very simple systems this procedure is usually not practical, and various approximate approaches to the problem are usually employed.

No practical, general method of solution is available when the optical roughness is large. However, for very simple systems, such as a wedge shaped groove [3], the methods of geometrical optics may be applied.

Several approaches have been used to determine the radiation properties when the optical roughness is small. A pertinent review of the literature with emphasis on diffraction theory is available in a text by Beckmann and Spizzichino [10]. A notable addition to the references in [10] is a paper by Porteus [11].

Before a method to determine the affect of roughness on the radiation properties can be selected, it is necessary to establish the range of optical

roughness of interest. The materials of primary interest in this investigation are those commonly used in the construction of spacecraft. Among these materials are the metals with surface roughnesses characteristic of those produced by normal machining, grinding and polishing operations. Typical surfaces produced by those operations have at most a mechanical root mean square (rms) roughness height of about one micron, with a half or a fourth micron probably more representative. For these surface roughnesses and for radiation in the infrared spectrum (.7 to 100 μ) the approximate range of optical roughness is .003 to 1. It is likely that diffraction effects will be the predominant influence on the radiation properties. This is probably true as well for radiation in the visible spectrum--solar radiation--at least for the smaller rms roughnesses of polished surfaces. In view of the range of optical roughnesses of interest, a diffraction model appears appropriate for describing the effects of roughness on the radiation properties of metals.

There is experimental evidence that the directional reflectance and hemispherical emittance are not appreciably affected by surface roughness when the optical roughness is small. On the other hand the spatial distribution of reflected energy is strongly influenced by surface roughness. Edwards and Catton [8] measured the normal spectral emittance and the spectral bi-directional reflectance of aluminum, titanium, and stainless steel samples which were roughened by common machining operations. They concluded that observed changes in emittance of a material for different surface preparations were probably due to surface damage, and not to shadowing and interreflection effects. Although the emittance was not appreciably affected, the spatial distribution of reflected energy was found very sensitive to surface roughness. Bennett [9] measured the monochromatic specular reflectance of ground glass coated with aluminum. These measurements were correlated with a model which

assumes no dependance of the directional reflectance on surface roughness. Contradictory experimental results may possibly be attributed to inadequate accounting of surface damage. Thus, it appears that at least for small optical roughnesses, a material with a rough surface possesses the same values of directional reflectance and hemispherical emittance as those of the same material with an optically smooth surface.

For surface profiles as complicated as those produced by machining operations on metals, the most practical method of accounting for diffraction effects appears to be Kirchhoff diffraction theory. The Maxwell equations are transformed into an integral equation, the Helmholtz integral, which requires knowledge of the electric field and its normal derivative at each point of the surface as well as the description of the surface contour for its solution. For engineering surfaces neither the field and its normal derivative nor the surface contour is known exactly, and appropriate assumptions must be made regarding their specification. Particular assumptions used by individual investigators concerning the electric field are summarized in [10]. The complicated roughness of engineering surfaces precludes an exact description of the surface contour, and a statistical description appears more appropriate.

Two diffraction models for the spectral bi-directional reflectance of rough metallic materials are described in Sections 2.1 and 2.2.

2.1 Beckmann's Bi-Directional Reflectance Model

2.1.1 Assumptions and Results

Since a detailed development of Beckmann's model is given in [10], only a brief discussion is given here. Beckmann considers reflection by a perfectly conducting material with random surface heights distributed according to the

Gaussian distribution with standard deviation σ. The two dimensional distribution function is Gaussian and the autocorrelation coefficient is taken exponential with correlation distance a. Physically, σ represents the rms roughness and a is proportional to the reciprocal of the rms slope of the surface profile. Interreflection and shadowing effects are neglected, and the analysis limited to ratios of correlation distance a to the incident wavelength λ much greater than unity ($a/\lambda >> 1$).

The result of the analysis for the bi-directional reflectance as defined in this report is (Refer to Figure 1)

$$f_\lambda(\psi,\pi;\ \theta,\phi) = f_{\lambda,c}(\psi)\ \delta(\theta - \psi)\ \delta(\phi - 0) + f_{\lambda,ic} \qquad (1)$$

where

$$f_{\lambda,c}(\psi) = \frac{\pi}{\cos\psi\ d\omega_i} \exp\left\{-(4\pi \frac{\sigma}{\lambda} \cos\psi)^2\right\} \qquad (2)$$

and

$$f_{\lambda,ic} = \frac{\pi^2 \left(\frac{a}{\lambda}\right)^2}{\cos\theta\ \cos\psi} \left(\frac{1 + \cos\theta\ \cos\psi - \sin\theta\ \sin\psi\ \cos\phi}{\cos\theta + \cos\psi}\right)^2 \cdot$$

$$\exp - \left\{2\pi \frac{\sigma}{\lambda} (\cos\theta + \cos\psi)\right\}^2 \cdot \sum_{m=1}^{\infty} \left\{ \frac{\left[(4\pi^2 (\frac{\sigma}{\lambda})^2 (\cos\theta + \cos\psi)^2\right]^m}{m\ m!} \right.$$

$$\left. \cdot \exp\left\{-\frac{\pi^2}{m}\left(\frac{a}{\lambda}\right)^2 [\sin^2\psi + \sin^2\theta - 2 \sin\psi \sin\theta \cos\phi]\right\} \right\} \qquad (3)$$

The subscripts c and ic denote coherent and incoherent respectively. The coherently reflected energy closely obeys the rules for purely specular reflection--angles of incidence and reflection are equal, and incident solid angle equals reflected solid angle. The solid angle of the incident beam is denoted by $d\omega_i$. Separation of the reflected energy into coherent and incoherent parts is a logical consequence of the derivation.

2.1.2 General Properties of the Model

The bi-directional reflectance is symmetric with respect to the plane of incidence, and it satisfies the Helmholtz reciprocity requirement. The coherent term depends only on the direction of the incident beam ψ and the optical roughness of the surface σ/λ for specified solid angle of incidence. On the other hand the incoherent part is influenced by the optical roughness, angle of incidence, direction of reflected beam, and the ratio of correlation distance to wavelength a/λ .

Figure 2 displays the coherent reflectance $(f_{\lambda,c}(\psi) \cos\psi \quad \frac{d\omega_i}{\pi})$ as a function of the optical roughness of the surface with angle of incidence ψ as a parameter. The coherent reflectance increases with increasing ψ for all values of optical roughness. In the limit as ψ approaches ninety degrees the coherent reflectance approaches unity independent of the optical roughness.

In Figure 3 the incoherent bi-directional reflectance is shown normalized with respect to the value in the direction of specular reflectance.

$$\frac{f_{\lambda,ic}(\psi,\pi,\ \theta,\phi)\ \cos\theta}{f_{\lambda,ic}(\psi,\pi,\ \psi,0)\ \cos\psi} \quad .$$

The angle of incidence is 10° and various combinations of the parameters σ/λ and a/λ are given. Results for $\phi = 0^\circ$ are shown on the right and those

for $\phi = 90^{\circ}$ on the left half of each graph. Maximum values occur for the specular direction and the reflectance diminishes with angular departure from this direction. The angular spread about the specular direction within which the bi-directional reflectance is significant diminishes rapidly with increasing values of a/λ for fixed σ/λ. The extent of the spread decreases with decreasing σ/λ. Similar trends occur for the other angles of incidence ψ, and the extent of the spread decreases with increasing ψ. The absolute bi-directional reflectance values $f_{\lambda,ic}(\psi,\pi;\theta,\phi)$ are presented in Tables 3 to 5 and are discussed later.

2.1.3 Radiant Energy Conservation

Since the reflecting material is assumed perfectly conducting, all incident energy must be accounted for in the reflected energy, that is, the directional reflectance must be unity. The directional reflectance, the fraction of the incident energy reflected for angle of incidence ψ, is obtained by multiplying (1) by $(\frac{\cos\theta \, d\omega_r}{\pi})$ and integrating over all reflected solid angles. From (1) the directional reflectance is

$$R_{\lambda}(\psi) = R_{\lambda,c} + R_{\lambda,ic} \tag{4}$$

where

$$R_{\lambda,c} = \exp -(4\pi \frac{\sigma}{\lambda} \cos\psi)^2 \tag{5}$$

is the fraction of the incident energy coherently reflected, and

$$R_{\lambda,ic} = \frac{1}{\pi} \int_0^{2\pi} \int_0^{\pi/2} f_{\lambda,ic} \cos\theta \sin\theta \, d\theta \, d\phi \tag{6}$$

is the fraction of the incident energy incoherently reflected.

The coherently reflected energy is dependent only on the angle of incidence and the optical roughness. If the incident energy is conserved, $R_\lambda(\psi)$ is unity and the incoherent directional reflectance is

$$R_{\lambda,ic} = 1 - R_{\lambda,c} = 1 - \exp\left\{-(4\pi\frac{\sigma}{\lambda}\cos\psi)^2\right\} \qquad (7)$$

It is apparent from (7) that the incoherently reflected energy also depends only on the optical roughness and angle of incidence. Hence, the parameter a/λ can only affect the spatial distribution and not the magnitude of the incoherently reflected energy. It is evident from Tables 3 to 5 that, with increasing a/λ, the incoherently reflected energy is confined to a diminishing solid angle about the specular direction for fixed σ/λ and ψ. That is, a surface of specified optical roughness, according to the model, exhibits an increasing specular reflectance with diminishing rms roughness slopes. Figures 6(a) and 6(b) are comparisons of data taken from [6] for which the optical roughnesses are nearly identical, but for which the reflectance distributions are quite different. Hence, it appears that the optical roughness by itself is not sufficient to characterize the spatial distribution of the reflected energy. This result is contradictory to statements made by Torrance and Sparrow [2].

The integration indicated in (6) was performed to determine the extent to which this model conforms to the energy conservation requirement for the parameter values of interest. Substitution and integration over ϕ gives

$$R_\lambda(\psi) = \left\{\exp\ -(4\pi\frac{\sigma}{\lambda}\cos\psi)^2\right\} + \frac{2\pi^2}{\cos\psi}\left(\frac{a}{\lambda}\right)^2 \sum_{m=1}^{\infty} \int_0^{\pi/2} \left\{\frac{\exp(-G)}{(\cos\theta+\cos\psi)^2}\right.$$

$$\left.\frac{G^m}{mm!}\exp(-F/m)\left[(A+C)\exp(-E/m)\ I_0(E/m) + (B-Hm)\exp(-E/m)\ I_1(E/m)\right]\sin\theta\,d\theta\right\} \qquad (8)$$

where

$$G = 4\pi^2 \left(\frac{\sigma}{\lambda}\right)^2 (\cos\theta + \cos\psi)^2$$

$$F = \pi^2 \left(\frac{a}{\lambda}\right)^2 (\sin\psi - \sin\theta)^2$$

$$E = 2\pi^2 \left(\frac{a}{\lambda}\right)^2 \sin\psi \sin\theta$$

$$D = -\pi^2 \left(\frac{a}{\lambda}\right)^2 (\sin^2\psi + \sin^2\theta)$$

$$B = -2 \sin\theta \sin\psi (1 + \cos\theta \cos\psi)$$

$$C = \sin^2\theta \sin^2\psi$$

$$A = (1 + \cos\theta \cos\psi)^2$$

$$H = C/E$$

$I_o(x)$; $I_1(x)$ are the modified Bessel functions of the first kind of order zero and one respectively for the argument x.

Equation (8) requires numerical integration. This was carried out for representative values of σ/λ between 0. and .5 . The numerical results are presented in Table 1 for selected values of ψ and a/λ . It was found that the directional reflectance is not unity in general. However, the deviation is usually less than 2%. For the smaller optical roughnesses, values of a/λ greater than or equal to one satisfy the conservation requirement. For optical roughness greater than .1 and for moderate angles of incidence, the conservation requirement is met only for larger values of a/λ . It remains for experiments to determine the values of a for engineering surfaces. Some information as to representative values of a can be obtained from the experiments performed by Birkebak [6]. Beckmann's model was used to correlate the measured reflectance distributions for optical roughnesses of about .1 . Values of a in the range 10 to 40 microns were obtained. These values of a are probably smaller than those which would

be produced by normal machining and polishing of metals. Thus, values of a of 50μ would not appear unlikely for engineering surfaces. Then, for wavelengths in the visible spectrum--which would also give the largest values of σ/λ --values of a/λ of 100 should not be unreasonable. It should be emphasized that measurements are necessary to determine the values of a characteristic of machined and polished metals.

In references [10], [12] it is suggested that the effect of the finite conductivity of engineering materials be accounted for by simply multiplying the bi-directional reflectance of a perfectly conducting material by the directional reflectance ($R_{\lambda,o}(\psi)$) of the actual material with an optically smooth surface. The bi-directional reflectance of an engineering material as predicted by this model is then,

$$\frac{\rho_\lambda(\psi, \pi; \theta, \phi)}{R_{\lambda,o}(\psi)} = f_{\lambda,c} + f_{\lambda,ic} \cdot \qquad (9)$$

In general this procedure is not expected to correctly account for finite conductivity; however, the difficulty of including this effect rigorously justifies the approximation at least until experiment proves it inadequate.

2.1.4 Experimental Verification

If this model is to be used in the planned comprehensive heat exchange calculations, it must predict reflectance distributions representative of metallic engineering materials.

Several investigators [6,9,12,4] have experimentally verified the coherent reflectance expression. It should be pointed out that the coherent term had been derived earlier. (Refer to [6] for a review of the literature.) Torrance and Sparrow [1] have used the coherent term to correlate their

specular reflectance measurements on nonconductors. Futher verification of the coherent term does not appear necessary.

Comprehensive measurements of the spectral bi-directional reflectance of rough metals for which quantitative surface descriptions are given appear limited to those of Birkebak [6]. Birkebak reports data for several ground nickel samples and ground glass samples coated with aluminum. The spectral bi-directional reflectance of each sample is measured for several wavelengths. Thus, reflectance distributions are reported for several optical roughnesses for each metal sample. Two samples, one ground glass coated with aluminum, and the second ground nickel, were selected as representative of the data. Figure 4 presents the data for the glass sample coated with aluminum for wavelengths of 1.5, 2., 4., 6., 8. μ, and Figure 5 that for the ground nickel sample for wavelengths of 2., 4., 6., 8. μ. Before the figures are discussed, the range of the parameters investigated by Birkebak should be pointed out. Reflectance measurements are reported for the optical roughness range of about .07 to 1.0 with $\psi = 10^{\circ}$. It is important to note that for $\psi = 10^{\circ}$ and $\sigma/\lambda \geq .15$, the measured relative specular reflectance of all the samples was less than .1 . Hence, in comparison to the total reflected energy, the energy reflected into the specular direction is quite small. Except for the limited data close to the specular direction, no bi-directional reflectance data is reported for the important range of optical roughnesses less than .15 . This range includes the more carefully machined and polished metals used in spacecraft exposed to infrared radiation.

Two important limitations of the available data for the verification of a diffraction model are apparent. First, a very important range of optical roughnesses has not been thoroughly investigated. Second, the affect of angle of incidence has not been studied except for the work of Torrance and Sparrow [2], which is almost entirely limited to $\sigma/\lambda > .4$. In view of these

conditions, thorough experimental verification of the model is not possible.

Beckmann's model was fit to the data for the aluminum sample, and the results are given on Figure 4 with Birkebak's data. The appropriate surface parameters were determined by a procedure outlined later in this section. The ordinate is the product of the bi-directional reflectance and $\cos\theta$ normalized to the corresponding value in the specular direction.

$$\left\{ \frac{\rho_\lambda (\psi,\pi;\ \theta,\phi)\ \cos\theta}{\rho_\lambda (\psi,\pi;\ \psi,0)\ \cos\psi} \right\} .$$

A similar procedure was used to develop Figure 5 for the nickel sample. The distribution for a Lambertonian surface is also included in Figure 4(a) for purposes of comparison.

For the distributions characterized by values of σ/λ of about .2 only qualitative agreement between theory and experiment is obtained. In the important range of σ/λ less than .2 insufficient data is reported to draw any definite conclusions. The fact that the data given for the smaller σ/λ ratios is insufficient is evident from that presented in Figure 4(e). The measured relative directional reflectance and relative specular reflectance for this case are respectively .91 and .34 . Because of the finite size of the detector, the peak shown represents roughly only that energy contained within the specular solid angle. Based on the measured directional reflectance, only ($.34/.91 \approx 38\%$) of the reflected energy is accounted for on this figure.

One important fact concerning the results presented in Figures 4 and 5 is also evident. Each of the surfaces should have unique values of a and σ. It is apparent from the values of a given for each of the two samples on these figures that this is essentially the situation for the smaller values of σ/λ.

However, for each sample it was necessary to reduce the value of a in order to fit the distributions for larger values of σ/λ . For these larger values of optical roughness, shadowing and interreflection effects increase in importance, and the applicability of the model becomes questionable. Probably the reduced values of a account for various approximations and limitations of the analysis for large optical roughnesses.

2.1.5 Approximate Result for Very Rough Surfaces

Beckmann has also given an approximate form of the general bi-directional reflectance expression when the coherent term is negligible. This condition is expressed in [10] as

$$4\pi^2 \left(\frac{\sigma}{\lambda}\right)^2 (\cos\theta + \cos\psi)^2 \gg 1 \qquad (10)$$

This approximation should apply to very rough surfaces for moderate angles of incidence. The expression--modified for finite conductivity--is

$$\frac{\rho_{ic}(\psi,\pi;\ \theta,\phi)}{R_{\lambda,o}(\psi)} = \left(\frac{a}{2\sigma}\right)^2 \frac{1}{\cos\theta\ \cos\psi} \left[\frac{1 + \cos\theta\ \cos\psi - \sin\theta\ \sin\psi\ \cos\phi}{(\cos\theta + \cos\psi)^2}\right]^2$$

$$\exp\left\{ -\left(\frac{a}{2\sigma}\right)^2 \frac{(\sin^2\theta + \sin^2\psi - 2\ \sin\psi\ \sin\theta\ \cos\phi)}{(\cos\theta + \cos\psi)^2} \right\} . \qquad (11)$$

An interesting point concerning this approximation is that it predicts a relative bi-directional reflectance independent of wavelength. This should be expected for roughness dimensions very large with respect to the wavelength. However, the application of a diffraction model which neglects shadowing and interreflections to such large optical roughness values is questionable.

At stated earlier, energy conservation requires that the relative

directional reflectance be unity. Numerical integration of (11) was carried out to obtain the relative directional reflectance. The results are presented in Figure 8. The relative directional reflectance $[R(\psi)/R_{\lambda,o}(\psi)]$ is plotted versus $(a/\sigma)^2$ for various values of incident angle ψ. The deviation from unity is less than about 1% for all angles of incidence between 0^o and 80^o if $(a/\sigma)^2$ is as large as 1000. Whether application of the model is valid for this range of the parameters remains to be determined from experiments.

In spite of the limitations given above this approximate form of the incoherent bi-directional reflectance can be used to correlate the data given by Birkebak for large values of σ/λ and $\psi = 10^o$. Figure 7 demonstrates this correlation. The solid line is the average of data taken from several surfaces all for large values of σ/λ. The vertical lines represent the spread of the data. The values of a/λ, σ/λ and a/σ obtained by fitting Beckmann's series solution to each case are also given on the figure. Beckmann's approximate solutions for $(a/\sigma)^2 = 32$ and 45 are also given. It should be emphasized that the values of a necessary to fit the data for each sample are considerably smaller than the corresponding values determined for the same surfaces but for smaller optical roughnesses (σ/λ). Again this is probably attributable to the use of the model outside of its expected range of validity.

2.1.6 Experimental Evaluation of σ and a

The experimental determination of σ and a can be accomplished with two specular reflectance measurements. As discussed here and by Bennett [9], for sufficiently long incident wavelength and reasonably small detector, the energy reflected into the specular direction is essentially all coherently

reflected. In this case the relative specular reflectance is from (5)

$$\frac{R_{\lambda,c}(SP)}{R_{\lambda,o}(\psi)} = \exp\left\{ -16\pi^2 \left(\frac{\sigma}{\lambda}\right)^2 \cos^2\psi \right\} \qquad (12)$$

If the relative specular reflectance is measured for known incident wavelength and angle of incidence, the only remaining unknown, σ, can be calculated.

If another relative specular reflectance measurement is made for a shorter wavelength, the incoherently reflected energy received by the detector cannot be neglected. The relative specular reflectance according to the model is then

$$\frac{R_{\lambda}(SP)}{R_{\lambda,o}(\psi)} = \frac{R_{\lambda,c}(SP) + R_{\lambda,ic}(SP)}{R_{\lambda,o}(\psi)} =$$

$$\exp\left\{-16\pi^2 \left(\frac{\sigma}{\lambda}\right)^2 \cos^2\psi\right\}\left[1 + d\omega_i \pi \left(\frac{a}{\lambda}\right)^2 \cos\psi \sum_{m=1}^{\infty} \frac{\left(16\pi^2 \left(\frac{\sigma}{\lambda}\right)^2 \cos^2\psi\right)^m}{m\, m\,!}\right] \qquad (13)$$

The only unknown is the desired parameter a since $\frac{R_{\lambda}(SP)}{R_{\lambda,o}(\psi)}$ was measured, ψ, λ, and the incident solid angle $d\omega_i$ are known, and σ was determined previously.

2.2 Davies' Bi-directional Reflectance Model

2.2.1 Assumptions and Results

Davies [5] considers the identical system as Beckmann but treats only the limiting cases of very small ($\sigma/\lambda << 1$) and very large ($\sigma/\lambda >> 1$) optical roughnesses. However, Beckmann [10] points out that the form of the Helmholtz integral used by Davies is strictly applicable only to plane

surfaces with apertures. Hence, the results should be expected to apply only to surfaces with very small profile slopes.

The bi-directional reflectance for $\sigma/\lambda << 1$ is

$$f_\lambda(\psi,\pi;\ \theta,\phi) = f_{\lambda,c}\ \delta(\theta - \psi)\ \delta(\phi-0) + f_{\lambda,ic} \qquad (14)$$

where

$$f_{\lambda,c} = \frac{\pi \exp\left\{-(4\pi \frac{\sigma}{\lambda} \cos\psi\ )^2\right\}}{\cos\psi\ \ d\omega_i}$$

and

$$f_{\lambda,ic} = \pi^4 \left(\frac{a}{\lambda}\right)^2 \left(\frac{\sigma}{\lambda}\right)^2 \frac{(\cos\theta + \cos\psi\ )^4}{\cos\theta\ \ \cos\psi}\ .$$

$$\exp\left\{-\pi^2 \left(\frac{a}{\lambda}\right)^2 [\sin^2\theta + \sin^2\psi - 2 \sin\theta\ \sin\psi\ \cos\phi\ ]\right\} \qquad (16)$$

This expression satisfies the reciprocity requirement, and the coherent term is identical to Beckmann's.

2.2.2 Radiant Energy Conservation

Since this model is for a perfectly conducting material all the incident energy must be reflected. Equation (14) was integrated over hemispherical space to obtain the directional reflectance. The results are presented in Table 2 for representative values of ψ, σ/λ, and a/λ. The results are quite striking in view of the common application of this model. The conservation requirement is satisfied only for very small optical roughnesses. In fact, the directional reflection is unity for all angles of incidence between 0° and 80° only for $\sigma/\lambda < .04$. For $\sigma/\lambda = .01$ only about 1% of the incident energy is not specularly reflected. A description of the spatial

distribution of the scattered energy appears of little importance from a practical viewpoint, since analyses based on purely specular reflection would appear sufficiently accurate.

It is apparent that this model is not satisfactory for the present application.

2.2.3 Approximate Result for $\sigma/\lambda >> 1$

The second solution given by Davies is for $\sigma/\lambda >> 1$. This appears questionable from the start since the initial form of the Helmholtz integral used was for plane surfaces. The result is--including corrections given in [7]--

$$f(\psi,\pi;\,\theta,\phi) = \frac{1}{16\cos\psi}\left(\frac{a}{\sigma}\right)^2 \exp\left\{-\left(\frac{a}{2\sigma}\right)^2\left[\frac{\sin^2\theta + \sin^2\psi - 2\sin\theta\,\sin\psi\,\cos\phi}{(\cos\theta + \cos\psi)^2}\right]\right\} \tag{17}$$

This equation was integrated to check the conservation requirement. The results are presented in Figure 8 with those for the corresponding approximation of Beckmann. The results show that the range of the parameter a/σ for which Davies' model satisfies the conservation requirement is indeed limited.

The limitations demonstrated in this section indicate that Davies' model is unsuitable for surfaces of interest in this investigation.

2.3 Conclusions

It has been demonstrated that the affect of surface roughness on the bi-directional reflectance of metals in the optical roughness range of interest ($\frac{\sigma}{\lambda} \gtrsim 1$) should be adequately described by a model based on diffraction theory. Two such models have been explored, namely those by Beckmann [10] and Davies [5].

Beckmann's result for bi-directional reflectance appears to satisfactorily describe the effects of surface roughness on the distribution of reflected energy. This model satisfies the requirements of reciprocity and energy conservation for important ranges of the controlling parameters. The coherent part, which is identical to Davies, has received extensive experimental verification, but only meager data is available to substantiate the incoherent part for an important range of optical roughness. Also, according to Beckmann's model and some experimental evidence, optical roughness is insufficient by itself to characterize the distribution of the reflected energy. The additional parameter required is related to the rms slope of the surface profile. Although the application of a result based on diffraction theory which neglects interreflection phenomena is questionable for large optical roughnesses, the approximate form of Beckmann's model for $\frac{\sigma}{\lambda} >> 1$ is physically reasonable for a wider range of the parameters than Davies'.

From the standpoint of accounting for the incident energy in the reflected beams for all angles of incidence, the Davies model for small optical roughnesses requires $\frac{\sigma}{\lambda}$ values less than 0.04. For optical roughnesses in the range ($\frac{\sigma}{\lambda} < 0.04$) almost all the incident energy is specularly reflected and heat exchange analyses based on purely specular reflection should be adequate.

3. PROPOSED FUTURE RESEARCH

The Beckmann bi-directional reflectance model appears to satisfactorily describe the distribution of reflected energy from rough metallic surfaces for the range of optical roughness typical of spacecraft surfaces. Evaluation of the radiant heat transfer may now proceed with confidence. Future efforts will be concentrated on the determination of the heat transfer rates and equilibrium temperature distribution for the proposed geometry [3] utilizing the Beckmann model. Related studies of the radiation properties of optically smooth surfaces will be completed and the results for other analyses of the effects of directional property variations on heat exchange submitted to NASA shortly.

4. REFERENCES

1. K. E. Torrance and E. M. Sparrow, "Biangular Reflectance of an Electric Nonconductor as a Function of Wavelength and Surface Roughness," Jour. of Heat Transfer, Trans. ASME, Series C, Vol. 87, 1965, pp. 283-292.

2. K. E. Torrance and E. M. Sparrow, "Off-Specular Peaks in the Directional Distribution of Reflected Thermal Radiation," ASME Paper, 65-WA/HT-19.

3. R. G. Hering, "Theoretical Study of Radiant Heat Exchange for Non-Gray, Non-Diffuse Surfaces in a Space Environment," Semi-Annual Status Report No. 1, NASA Research Grant, No. NGR-14-005-036.

4. H. E. Bennett, "Specular Reflectance of Aluminized Ground Glass and the Height Distribution of Surface Irregularities," Jour. Opt. Soc. Am., Vol. 53, No. 12, Dec. 1963, pp. 1389-1394.

5. H. Davies, "The Reflection of Electromagnetic Waves from a Rough Surface," Proc. I.E.E., Pt. III, Vol. 101, 1954, pp. 209-214.

6. R. C. Birkebak, "Monochromatic Directional Distribution of Reflected Thermal Radiation from Roughened Surfaces," Ph.D. Dissertation, Mechanical Engineering Department, University of Minnesota, Minneapolis, Minnesota, September 1962.

7. L. M. Spetner, "Discussion of [5], Proc. I.E.E., Pt. III, Vol. 102, 1955, pp. 148.

8. D. K. Edwards and I. Catton, "Radiation Characteristics of Rough and Oxidized Metals," Symposium on Thermophysical Properties, Held at Purdue University, 1965.

9. H. E. Bennett, "Influence of Surface Roughness, Surface Damage, and Oxide Films on Emittance," Symposium on Thermal Radiation of Solids, NASA SP-55, 1965, pp. 145-152.

10. P. Beckmann and A. Spizzichino, "The Scattering of Electromagnetic Waves from Rough Surfaces," The Macmillan Company, New York, 1963.

11. J. O. Porteus, "Relation Between Height Distribution of a Rough Surface and the Reflectance at Normal Incidence," Jour. Opt. Soc. Am., Vol. 53, No. 12, Dec. 1963, pp. 1394-1402.

12. H. E. Bennett and J. O. Porteus, "Relation Between Surface Roughness and Specular Reflectance at Normal Incidence," Jour. Opt. Soc. Am., Vol. 51, No. 2, Feb. 1961, pp. 123-129.

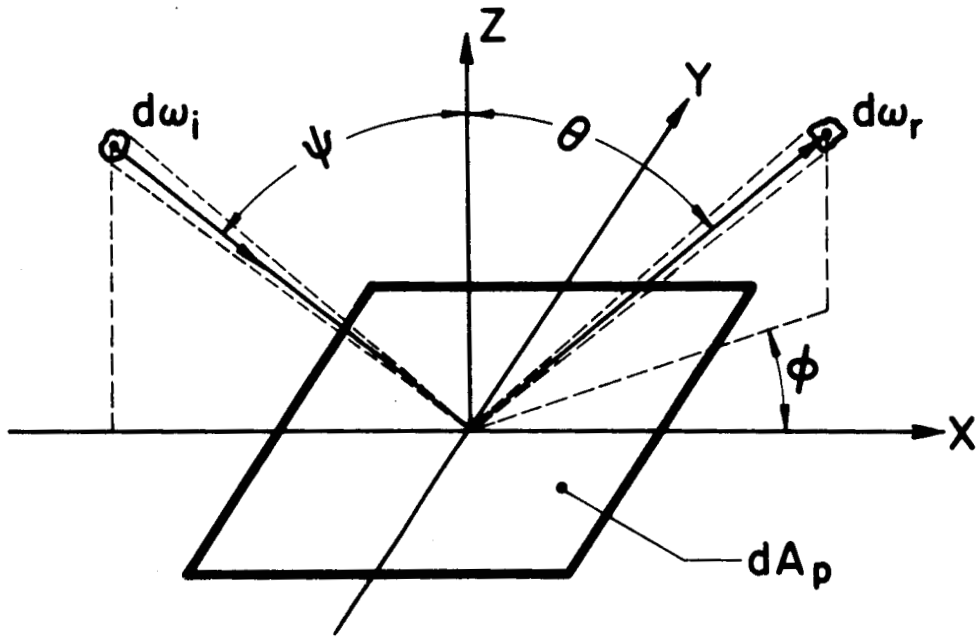

FIG. 1 ANGLES OF INCIDENCE AND REFLECTION.

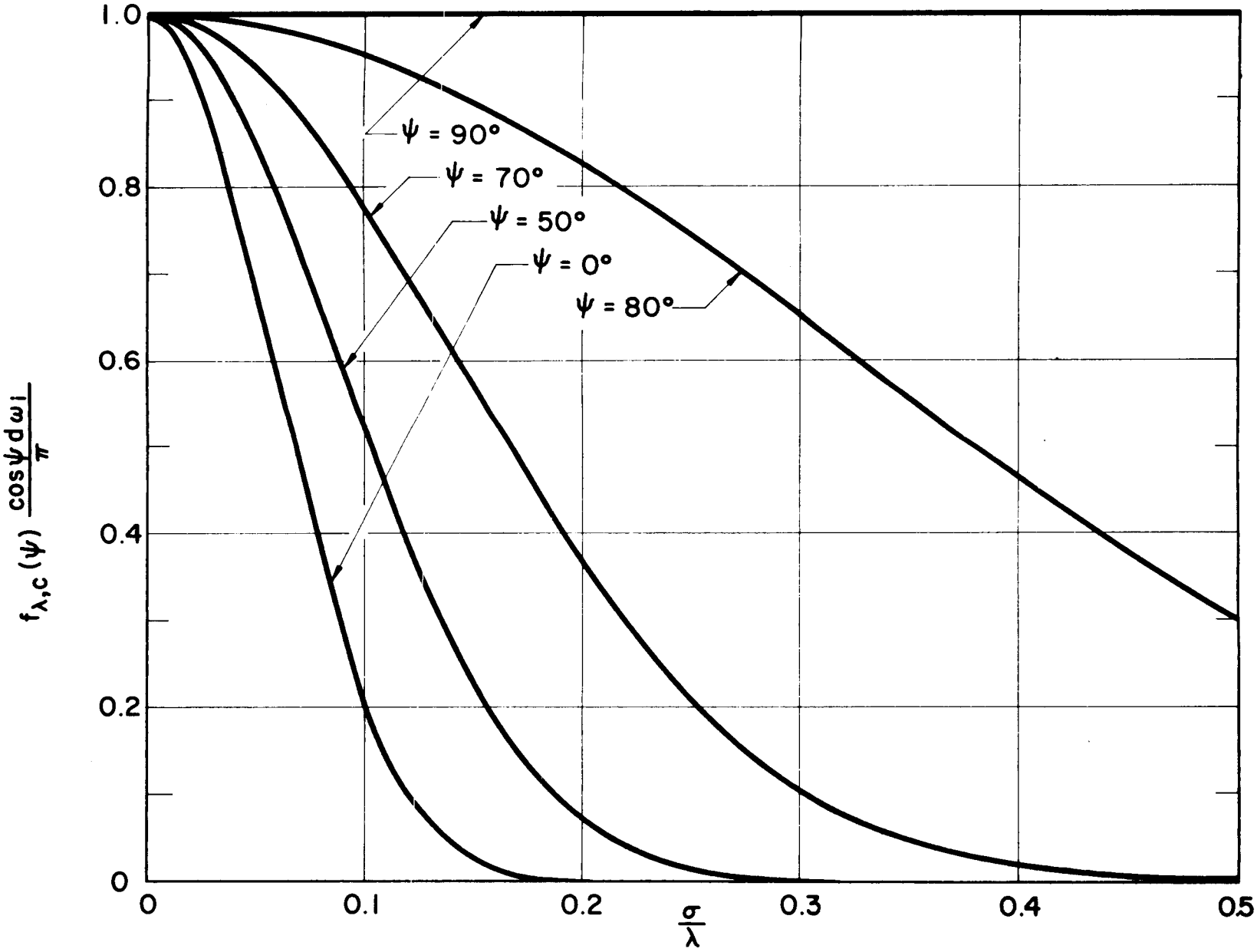

FIG. 2 COHERENT REFLECTANCE FROM BECKMANN'S MODEL.

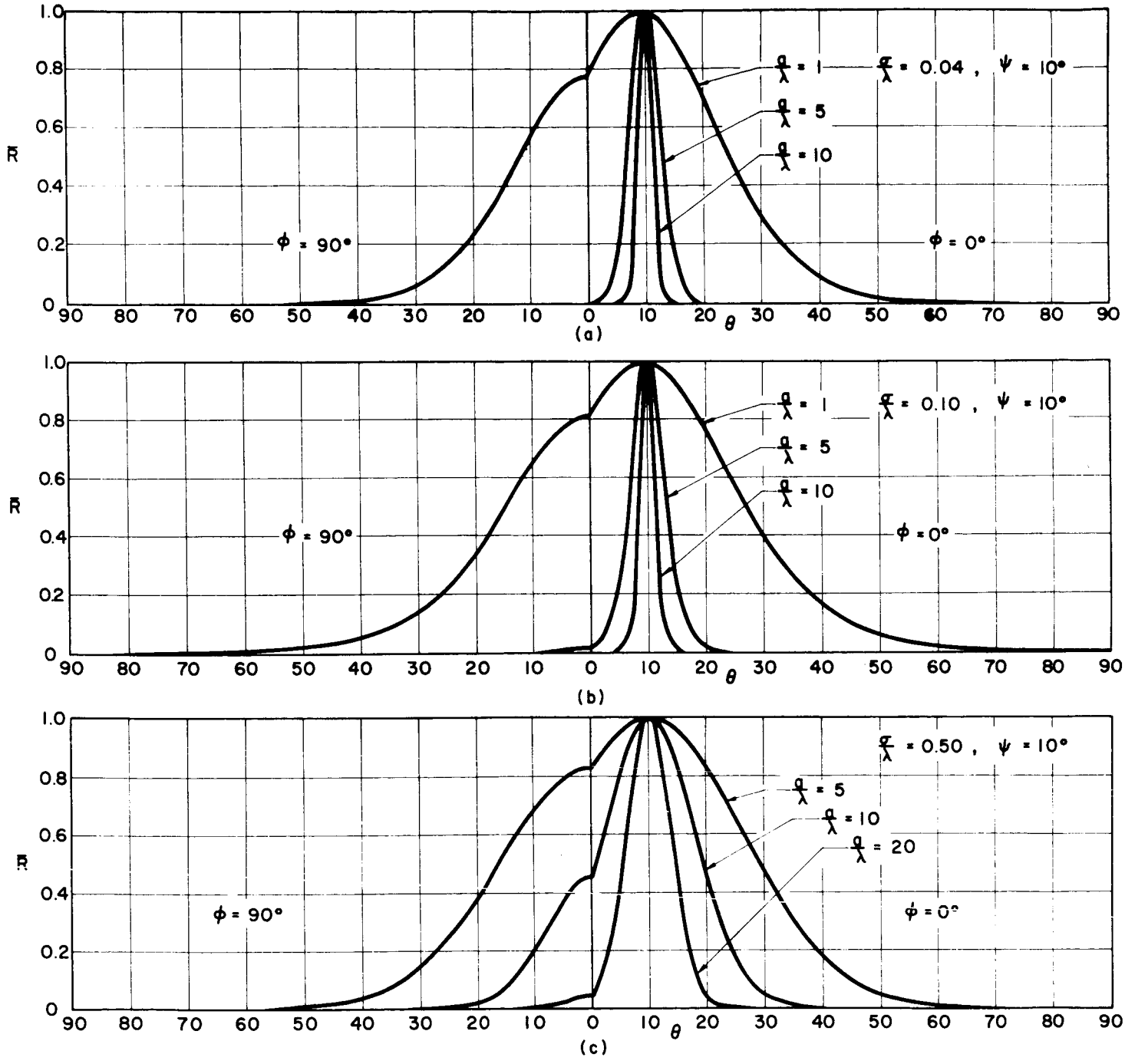

FIG. 3 NORMALIZED INCOHERENT BI-DIRECTIONAL REFLECTANCE FROM BECKMANN'S MODEL.

$$\bar{R} = f_{\lambda,ic}(\psi, \pi; \theta, \phi)\cos\theta \Big/ f_{\lambda,ic}(\psi, \pi; \psi, o)\cos\psi$$

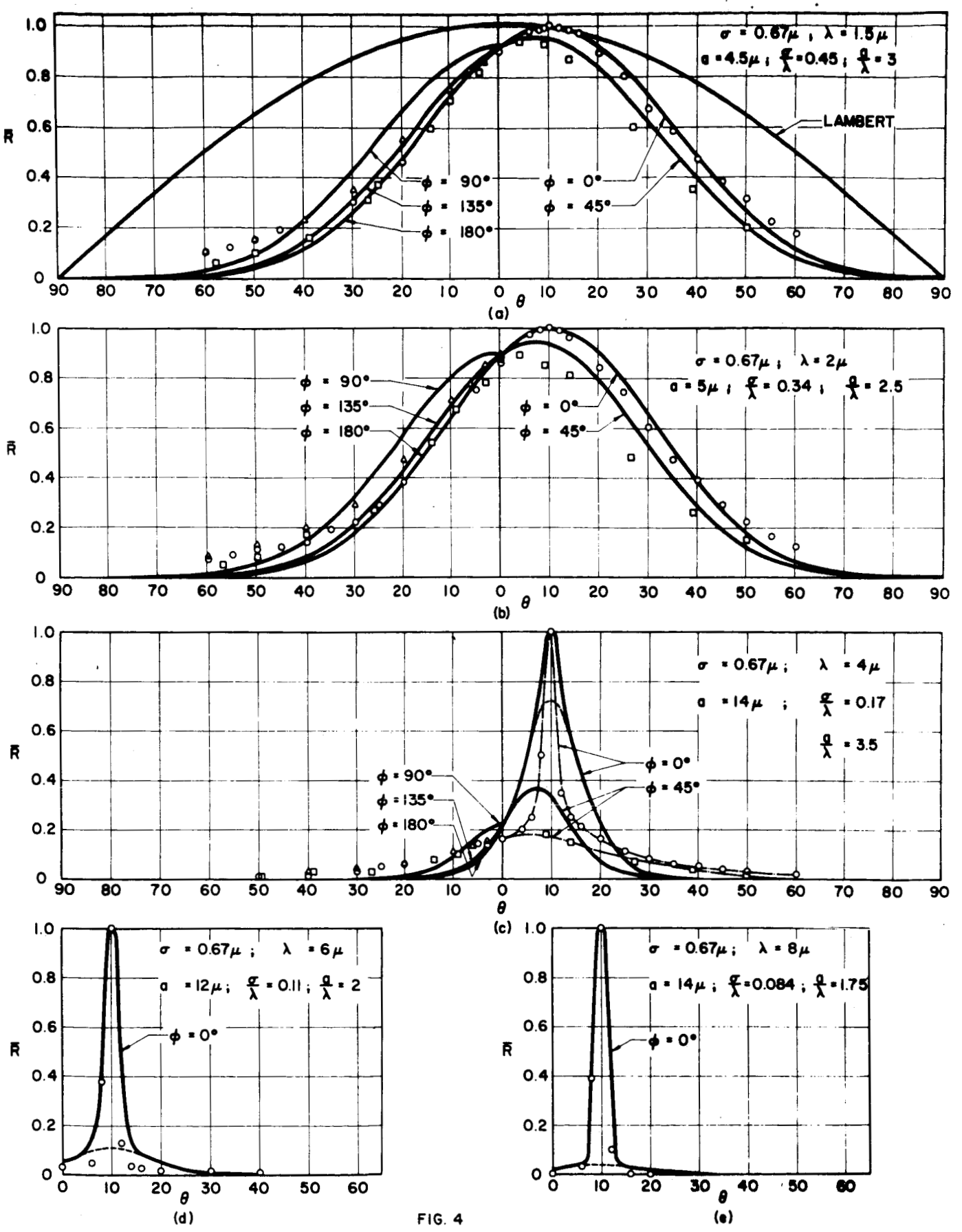

FIG. 4

COMPARISON OF BECKMANN'S MODEL WITH BIRKEBAK'S DATA

(DATA FOR GROUND GLASS AL. COATED ; REF. [6] ; $\sigma = 0.67\mu$; $\psi = 10°$)

——— SUM OF COHERENT AND INCOHERENT COMPONENTS.

- - - - - - - INCOHERENT COMPONENT.

——·—— CURVE CONNECTING DATA.

$$\bar{R} = \rho_\lambda(\psi, \pi; \theta, \phi)\cos\theta \,/\, \rho_\lambda(\psi, \pi; \psi, 0)\cos\psi$$

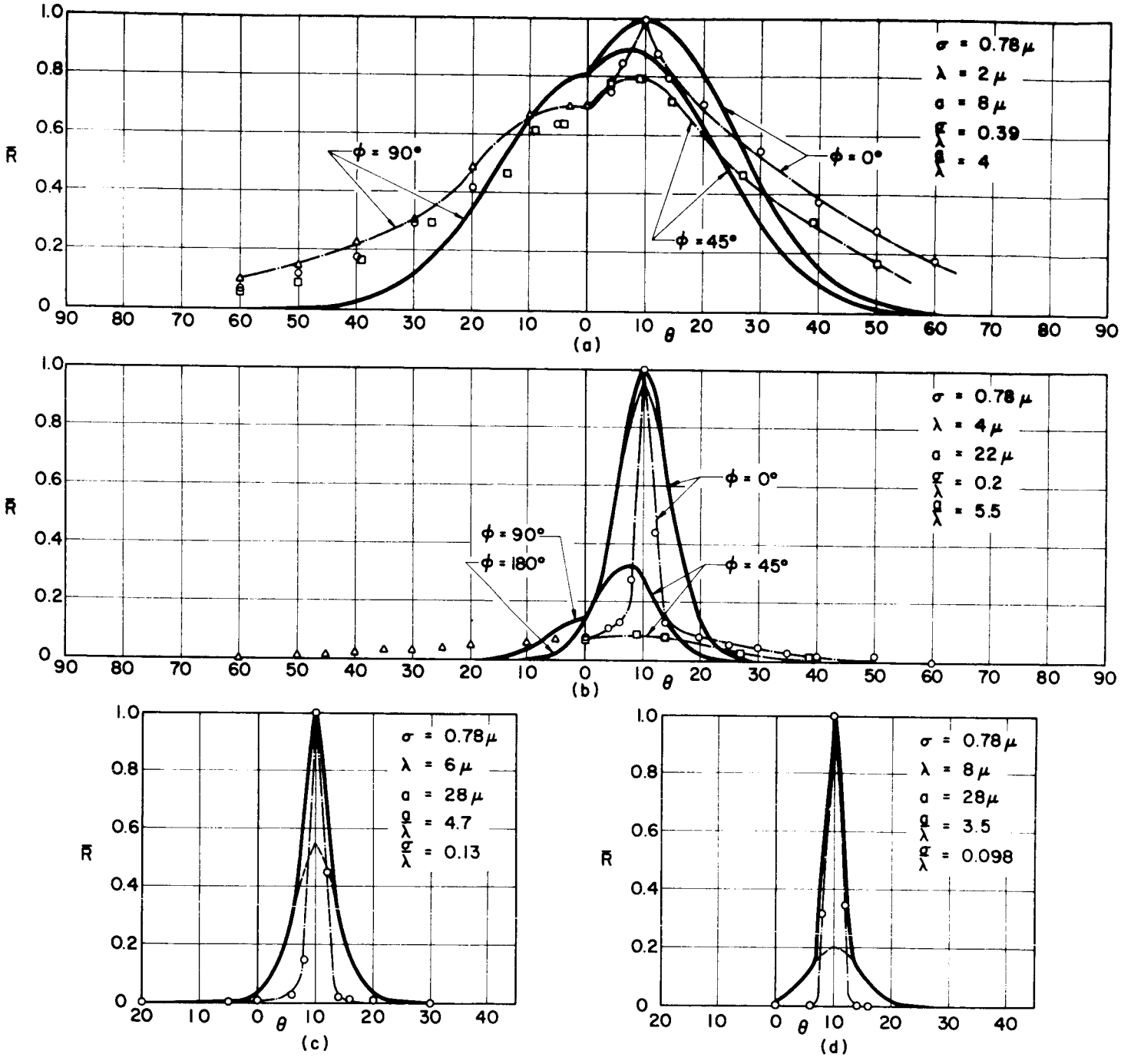

FIG. 5 COMPARISON OF BECKMANN'S MODEL WITH BIRKEBAK'S DATA (DATA FOR GROUND NICKEL , REF. [6] , $\sigma = 0.78\mu$; $\psi = 10°$)

——— SUM OF COHERENT AND INCOHERENT COMPONENTS.

- - - - - - - INCOHERENT COMPONENT.

——·—·—— CURVE CONNECTING DATA.

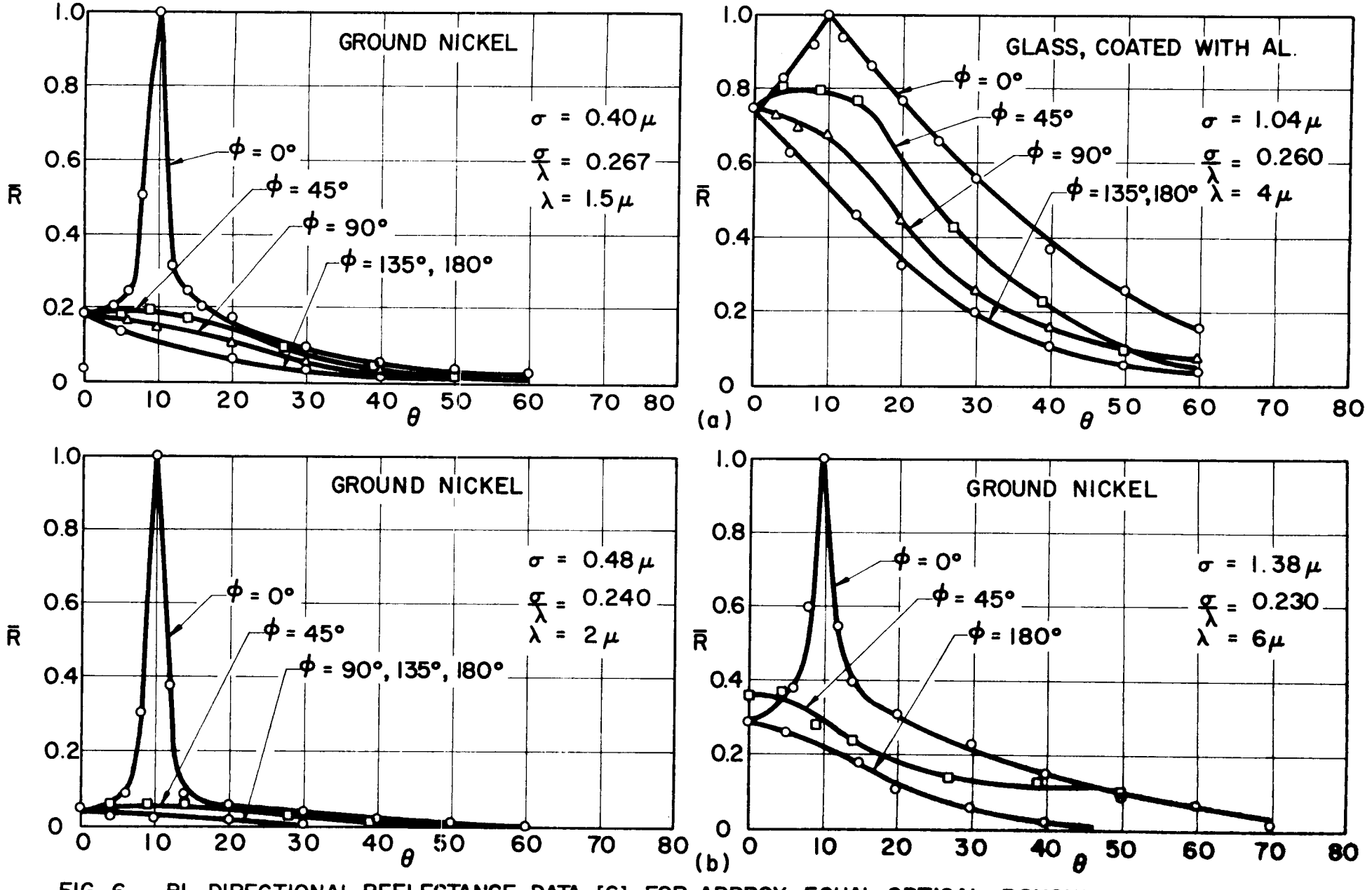

FIG. 6 BI-DIRECTIONAL REFLECTANCE DATA [6] FOR APPROX. EQUAL OPTICAL ROUGHNESS VALUES.

$$\bar{R} \equiv \rho_\lambda(\psi, \pi; \theta, \phi) \cos\theta / \rho_\lambda(\psi, \pi; \psi, o) \cos\psi$$

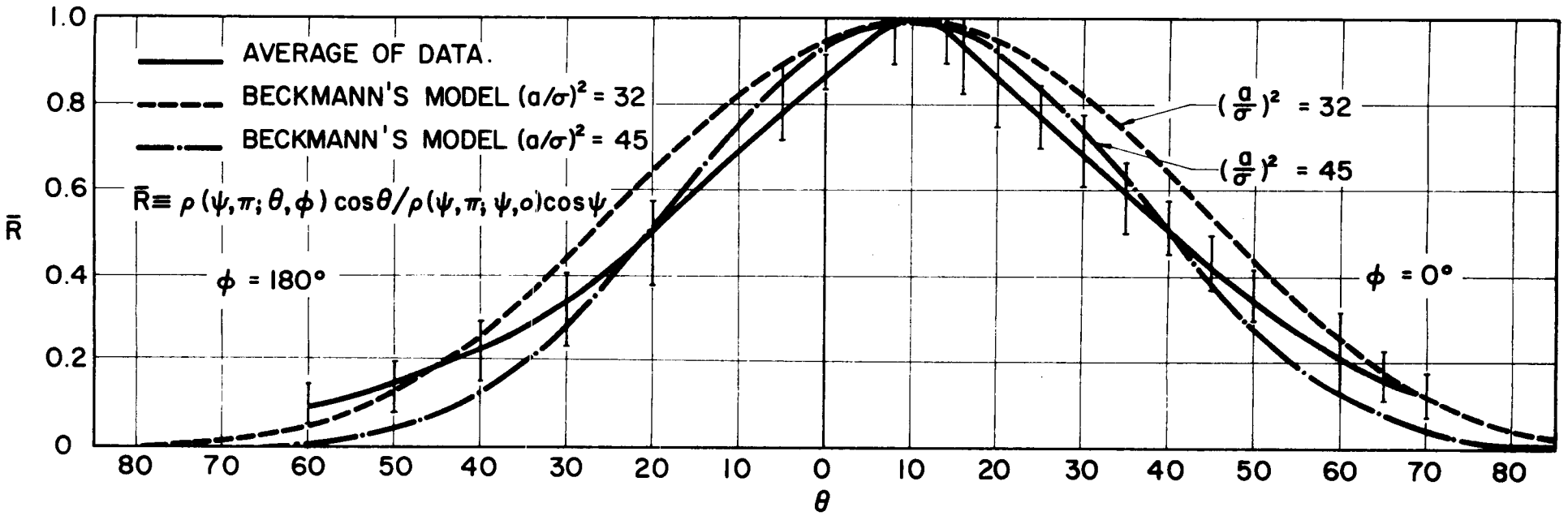

FIG. 7 COMPARISON OF BECKMANN'S MODEL WITH DATA [6] FOR LARGE OPTICAL ROUGHNESS.

MATERIAL	$\sigma(\mu)$	$\lambda(\mu)$	σ/λ	a/σ	a/λ
AL.	0.67	1.5	0.45	6.7	3.0
AL.	0.58	1.0	0.58	6.9	4.0
AL.	1.04	2.0	0.52	5.8	3.0
AL.	1.01	2.0	0.51	6.9	3.5
AL.	2.06	4.0	0.52	5.8	3.0
NI.	1.38	2.0	0.69	5.8	4.0

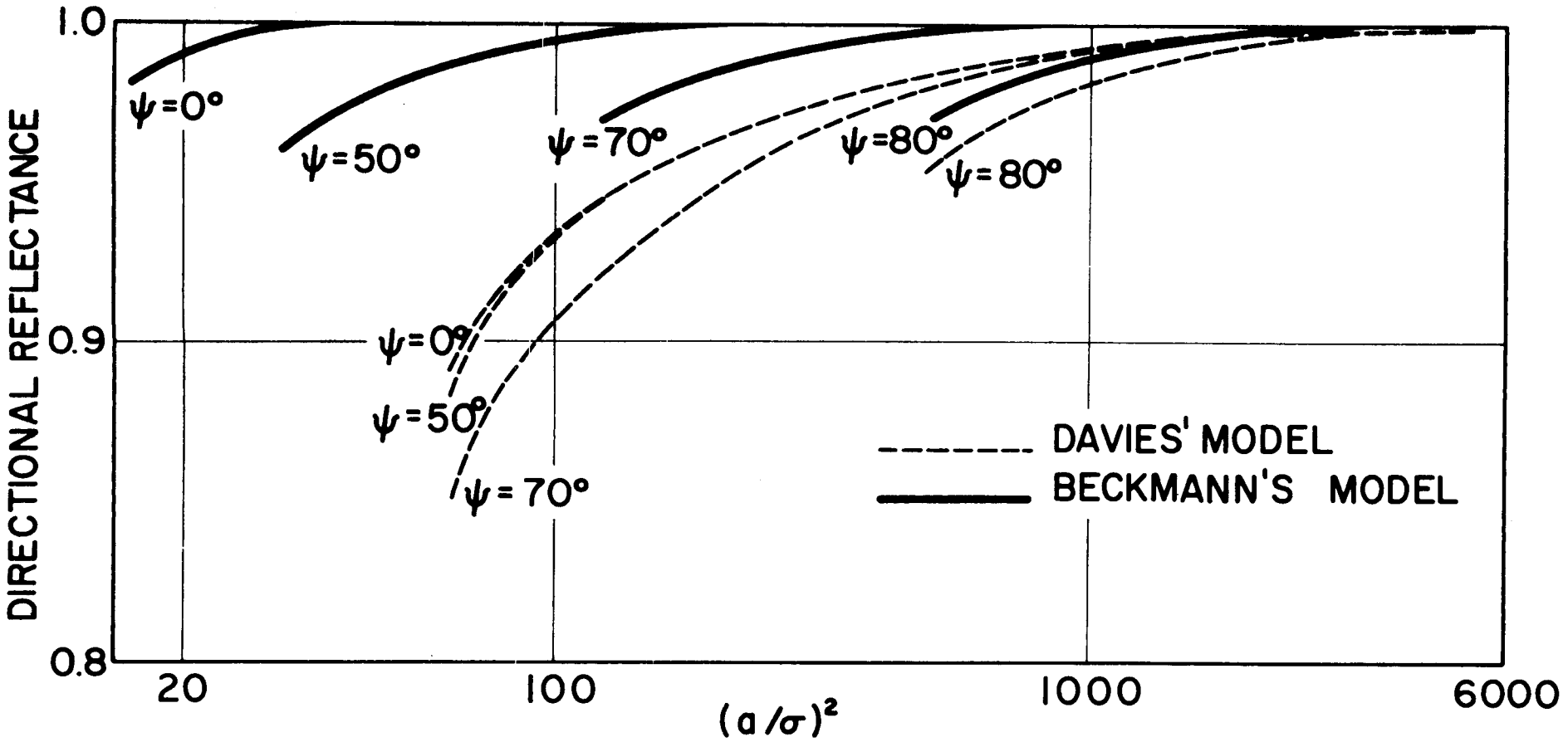

FIG. 8 DIRECTIONAL REFLECTANCE FOR LARGE OPTICAL ROUGHNESS.

TABLE 1

Directional Reflectance from Beckmann's Model

$\frac{\sigma}{\lambda} = 0.01$					
ψ	a/λ				
	1.	5.	10.	50.	100.
0°	1.000	1.000	1.000	1.000	1.000
40°	1.000	1.000	1.000	1.000	1.000
80°	1.002	1.000	1.000	1.000	1.000

$\frac{\sigma}{\lambda} = 0.04$					
ψ	a/λ				
	1.	5.	10.	50.	100.
0°	1.000	1.000	1.000	1.000	1.000
40°	0.996	1.000	1.000	1.000	1.000
80°	1.025	1.002	1.000	1.000	1.000

$\frac{\sigma}{\lambda} = 0.08$					
ψ	a/λ				
	1.	5.	10.	50.	100.
0°	--	0.996	1.000	1.000	1.000
40°	0.984	0.997	0.997	0.997	0.997
80°	--	1.006	1.000	1.000	1.000

$\frac{\sigma}{\lambda} = 0.16$					
ψ	a/λ				
	1.	5.	10.	50.	100.
0°	0.996	1.000	1.000	1.000	1.000
40°	0.960	1.000	1.000	1.000	1.000
80°	1.351	1.022	0.999	1.000	1.000

TABLE 1. Cont'.

$\frac{\sigma}{\lambda} = 0.20$					
ψ	a/λ				
	5.	10.	20.	50.	100.
0°	1.000	1.000	1.000	1.000	1.000
40°	1.000	1.000	1.000	1.000	1.000
80°	1.032	0.997	0.996	1.000	1.000

$\frac{\sigma}{\lambda} = 0.50$					
ψ	a/λ				
	10.	20.	100.	150.	
0°	1.000	1.000	1.000	1.000	
40°	1.000	1.000	1.000	1.000	
80°	0.980	0.978	0.998	0.999	

TABLE 2

Directional Reflectance from Davies' Model

$\frac{\sigma}{\lambda} = 0.01$					
ψ	a/λ				
	1.	5.	10.	50.	100.
0°	0.999	1.000	1.000	1.000	1.000
40°	0.999	1.000	1.000	1.000	1.000
80°	1.000	1.000	1.000	1.000	1.000

$\frac{\sigma}{\lambda} = 0.04$					
ψ	a/λ				
	1.	5.	10.	100.	
0°	1.017	1.029	1.029	1.029	
40°	0.995	1.010	1.010	1.011	
80°	1.015	1.001	1.000	1.000	

$\frac{\sigma}{\lambda} = 0.10$					
ψ	a/λ				
	1.	5.	10.	50.	100.
0°	1.705	1.782	1.785	1.785	1.785
40°	1.226	1.319	1.322	--	1.323
80°	1.094	1.009	1.000	1.001	1.001

$\frac{\sigma}{\lambda} = 0.16$					
ψ	a/λ				
	1.	5.	10.	50.	100.
0°	3.855	4.052	4.058	4.060	4.060
40°	2.218	2.457	2.464	2.466	2.466
80°	1.245	1.027	1.005	1.007	1.007

TABLE 2. Cont'.

$\frac{\sigma}{\lambda} = 0.20$					
Ψ	a/λ				
	1.	5.	10.	50.	100.
0°	5.999	6.306	6.315	6.318	6.318
40°	--	3.719	3.728	3.731	3.731
80°	1.389	1.048	1.013	1.017	1.017

$\frac{\sigma}{\lambda} = 0.50$					
Ψ		a/λ			
	10.	20.	100.	150.	
0°	39.46	39.47	39.48	39.48	
40°	23.15	23.16	23.17	23.17	
80°	1.470	1.462	1.494	1.494	

TABLE 3

Absolute Bi-Directional Reflectance
from Beckmann's Model

$$f_{\lambda,ic}(\psi,\pi;\theta,\phi)\cos\theta$$

$$\psi = 10^{\circ};\ \phi = 0^{\circ};\ \frac{\sigma}{\lambda} = 0.04$$

θ°	a/λ		
	1.	5.	10.
0	1.555	0.117	0.589 - 4
4	1.843	4.199	0.835 - 1
8	1.983	1.637 + 1	0.652 + 2
10	1.985	4.962 + 1	0.198 + 3
12	1.940	3.706 + 1	0.646 + 2
16	1.729	4.259 + 0	0.904 - 1
20	1.412	0.131	0.806 - 4
24	1.064	0.460 - 2	0.597 - 7
28	0.746	0.150 - 3	0.413 - 10
32	0.491	0.498 - 5	0.290 - 13
36	0.307	0.172 - 6	0.221 - 16
40	0.185	0.626 - 8	0.193 - 19
44	0.108	0.247 - 9	0.204 - 22
48	0.624 - 1*	0.108 - 10	0.274 - 25
52	0.358	0.534 - 12	0.484 - 28
56	0.208	0.303 - 13	0.118 - 30
60	0.122	0.202 - 14	0.395 - 33
64	0.737 - 2	0.160 - 15	---
68	0.458	0.155 - 16	---
72	0.295	0.184 - 17	---
76	0.198	0.273 - 18	---
80	0.139	0.515 - 19	---
84	0.102	0.125 - 19	---
88	0.786 - 3	0.396 - 20	---
90	0.704 - 3	0.247 - 20	---

* denotes 0.624×10^{-1}

TABLE 4

Absolute Bi-Directional Reflectance
from Beckmann's Model

$$f_{\lambda,ic}(\psi,\pi;\theta,\phi)\cos\theta$$

$$\psi = 10^{\circ};\ \phi = 0^{\circ};\ \frac{\sigma}{\lambda} = 0.10$$

θ°	a/λ		
	1.	5.	10.
0	4.105	2.496	0.256 - 1
4	4.706	2.071 + 1	3.277 + 0
8	5.011	1.004 + 2	2.100 + 2
10	5.028	1.257 + 2	5.028 + 2
12	4.951	9.943 + 1	2.089 + 2
16	4.547	2.062 + 1	3.339 + 0
20	3.899	2.528 + 0	0.289 - 1
24	3.142	0.274	0.175 - 3
28	2.401	0.264 - 1	0.852 - 6
32	1.755	0.238 - 2	0.367 - 8
36	1.241	0.205 - 3	0.150 - 10
40	0.856	0.174 - 4	0.618 - 13
44	0.582	0.149 - 5	0.269 - 15
48	0.393	0.130 - 6	0.129 - 17
52	0.264	0.119 - 7	0.712 - 20
56	0.178	0.116 - 8	0.470 - 22
60	0.121	0.123 - 9	0.386 - 24
64	0.826 - 1	0.143 - 10	0.407 - 26
68	0.570	0.187 - 11	0.571 - 28
72	0.399	0.277 - 12	0.110 - 29
76	0.283	0.476 - 13	0.301 - 31
80	0.205	0.959 - 14	0.120 - 32
84	0.151	0.230 - 14	0.619 - 34
88	0.114	0.668 - 15	---
90	0.101	0.388 - 15	---

TABLE 5

Absolute Bi-Directional Reflectance
from Beckmann's Model

$$f_{\lambda,ic}(\psi,\pi;\theta,\phi)\ \cos\theta$$

$$\psi = 10^{\circ};\ \phi = 0^{\circ};\ \frac{\sigma}{\lambda} = 0.50$$

θ°	a/λ		
	5.	10.	20.
0	5.410	1.191 + 1	4.781
4	6.097	1.964	3.349 + 1
8	6.472	2.527	9.179 + 1
10	6.522	2.609	1.043 + 2
12	6.474	2.528	9.182 + 1
16	6.102	1.965	3.347 + 1
20	5.416	1.190	4.779 + 0
24	4.524	5.649 + 0	0.299
28	3.552	2.121	0.922 - 2
32	2.619	0.637	0.156 - 3
36	1.811	0.155	0.158 - 5
40	1.173	0.309 - 1	0.105 - 7
44	0.711	0.513 - 2	0.491 - 10
48	0.403	0.722 - 3	0.173 - 12
52	0.214	0.874 - 4	0.486 - 15
56	0.106	0.929 - 5	0.117 - 17
60	0.494 - 1	0.882 - 6	0.254 - 20
64	0.216	0.766 - 7	0.531 - 23
68	0.891 - 2	0.622 - 8	0.114 - 25
72	0.349	0.483 - 9	0.264 - 28
76	0.131	0.369 - 10	0.711 - 31
80	0.471 - 3	0.286 - 11	0.236 - 33
84	0.166	0.231 - 12	0.103 - 35
88	0.575 - 4	0.201 - 13	---
90	0.339 - 4	0.615 - 14	---